© 2014. Published by The Company of Biologists Ltd | Journal of Cell Science (2014) 127, 3104–3115 doi:10.1242/jcs.145854

RESEARCH ARTICLE

Lipid droplet formation in response to oleic acid in Huh-7 cells is mediated by the fatty acid receptor FFAR4

Arndt Rohwedder*, Qifeng Zhang, Simon A. Rudge and Michael J. O. Wakelam‡

ABSTRACT

It is unclear how changes in lipid droplet size and number are regulated – for example, it is not known whether this involves a signalling pathway or is directed by cellular lipid uptake. Here, we show that oleic acid stimulates lipid droplet formation by activating the long-chain fatty acid receptor FFAR4, which signals through a pertussis-toxin-sensitive G-protein signalling pathway involving phosphoinositide 3-kinase (PI3-kinase), AKT (also known as protein kinase B) and phospholipase D (PLD) activities. This initial lipid droplet formation is not dependent upon exogenous lipid, whereas the subsequent more sustained increase in the number of lipid droplets is dependent upon lipid uptake. These two mechanisms of lipid droplet formation point to distinct potential intervention points.

KEY WORDS: Lipid droplets, Oleic acid, PI3-kinase, Phospholipase D, FFAR4, Fatty acid receptor

INTRODUCTION

Lipid droplets are intracellular storage organelles found in most cells in essentially all organisms (Athenstaedt et al., 1999; Wan et al., 2007; Fujimoto et al., 2008). Lipid droplets are made up of a core of neutral lipids (Zweytick et al., 2000; Cheng et al., 2009) surrounded by a monolayer of phospholipids (Tauchi-Sato et al., 2002; Fujimoto and Ohsaki, 2006) in which is embedded a unique set of proteins (Goodman, 2009; Walther and Farese, 2009; Hodges and Wu, 2010; Meex et al., 2009). Lipid droplets are highly dynamic organelles, and the application of long-chain fatty acids generates droplets in most cell types (Schadinger et al., 2005; Fujimoto et al., 2006). Extensive generation of these neutral lipid storage organelles has been implicated in a number of diseases, including non-alcoholic steatohepatitis (NASH) (Anderson and Borlak, 2008; Neuschwander-Tetri, 2010), obesity and type 2 diabetes (Agarwal and Garg, 2006; Thiele and Spandl, 2008; Boström et al., 2009). Dysregulation of the formation of lipid droplets also affects the process of atherosclerosis (Paul et al., 2008). In addition, lipid droplets are important in infection by hepatitis type C virus (HCV); a capsid (core) and a non-structural protein (NS5A) are targeted to lipid droplets, resulting in HCV particles assembling at lipid droplets – indeed, disturbance of lipid droplet targeting can suppress HCV production (Sato et al., 2006; Fujimoto et al., 2008; Clément et al., 2011).

The excessive accumulation of intracellular lipid droplets can have further implications. In Chanarin-Dorfman syndrome, triacylglycerol, a major lipid constituent of lipid droplets, is deposited and stored in different tissues, but not in adipose tissue (Fujimoto et al., 2008). Lipodystrophy is marked by a loss of adipose tissue in Berardinelli-Seip congenital lipodystrophy 2 (BSCL2) (Boutet et al., 2009), associated with a reduction or defect in the sorting of caveolin-1 (Blouin et al., 2010). The control of lipid droplet generation, composition and turnover is therefore important for cells. However, it remains unclear whether this regulation is brought about through an externally activated signalling pathway or is just directed by cellular lipid availability and, thus, uptake (Digel et al., 2010). It has been suggested that the formation, localisation and growth of lipid droplets is dependent upon phospholipase D (PLD) and the ERK pathway (Nakamura et al., 2005; Andersson et al., 2006) but, despite this, the involvement of signalling pathways in the stimulated formation of lipid droplets in response to cell exposure to fatty acids, an indicator of nutritional uptake, is unclear. In order to investigate this, the hepatoma cell line Huh-7 was examined as a model of hepatic lipid uptake. Under normal conditions, this cell line contains a high number of lipid droplets of an intermediate average size, and the cells can be used to represent hepatic conditions. The results presented in this paper provide evidence that long-chain fatty acids increase lipid droplet formation through both an acute fatty-acid-receptor-mediated signalling pathway and a longer lasting lipid-uptake-mediated pathway.

RESULTS

Depletion of fatty acids from cell culture medium by overnight serum withdrawal brought about an ~85% reduction in the number of detectable lipid droplets in Huh-7 cells; this could be reversed by the addition of 100 µM oleate to the serum-free medium (Fig. 1). This increase in the number of lipid droplets was apparent within a few minutes after the addition of oleate (Fig. 1) and was concentration dependent. The increase in lipid droplet number following oleate addition was a biphasic process; the rapid increase from the starvation level was observable by 5 min after oleate addition (the fold increase above the starved control was 1.44±0.17; ±s.e.m.) and increased up to 30 min (3.13±0.24), followed by a plateau phase to ~60 min (3.23±0.24), after which there followed a continuous increase in lipid droplet number (120 min, 3.88±0.18; 180 min, 4.92±0.19) (Fig. 1E). In control untreated cells, the fold elevation in the number of droplets per cell compared with that of the starved condition was 7.95±0.37. Oleate-stimulated droplet formation was ablated in pertussis-toxin-treated cells (Fig. 1F).

Signalling Programme, Babraham Institute, Babraham Research Campus, Cambridge CB22 3AT, UK.
*Present address: Christian-Albrechts-Universität zu Kiel, MOIN-CC, Am Botanischen Garten 14, 24118 Kiel, Germany.

‡Author for correspondence (Michael.wakelam@babraham.ac.uk)

Received 6 November 2013; Accepted 26 April 2014

Journal of Cell Science

Journal of Cell Science (2014) 127, 3104–3115 doi:10.1242/jcs.145854

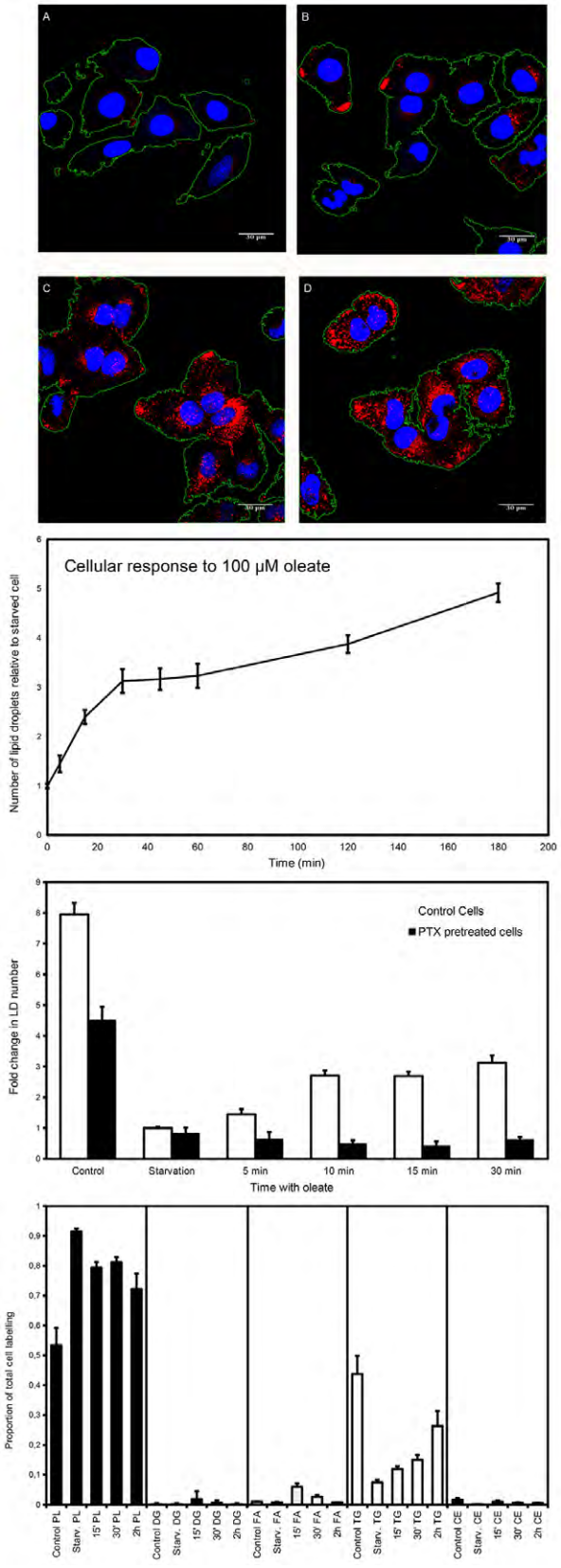

Fig. 1. Oleate-stimulated increase in lipid droplets in Huh-7 cells. (A–D) Maximum projection of 3D confocal recordings of Huh-7 cells in which lipid droplets have been stained with the LD540 dye (red) and nuclei have been stained with Hoechst 33342 (blue). Cell outlines are shown in green. Cells were starved for 16 h (A), and this was followed by incubation with 100 μM oleate for 15 min (B) or 3 h (C). Control Huh-7 cells grown in complete medium are also shown (D). Scale bars: 30 μm. (E) Quantification of lipid droplets in oleate-exposed cells from the 3D confocal imaging. Data represent the mean±s.e.m. and were normalised to results from serum-starved cells. (F) Oleate-stimulated lipid droplet (LD) formation was inhibited by pretreating Huh-7 cells with 10 ng/ml pertussis toxin (PTX) for 16 h during the starvation period. Data show the mean±s.e.m. (G) Relative distribution of [^{3}H]-oleate in lipids from Huh-7 cells that were incubated with 1 μCi of [^{3}H]-oleic acid in DMEM for 1 h before being stimulated with 100 μM oleate; the cells had been cultured serum-free for 16 h prior to the experiments (Starv). The proportion of radiolabel in each fraction was determined as described in Materials and Methods. Data are presented as means of the proportion of disintegrations per minute in each fraction (±s.d.). P, phospholipids; DG, diacylglycerol; FA, fatty acids; TG, triglycerides; CE, cholesterol ester.

This two-phase process suggests the involvement of distinct mechanisms. To examine stimulated changes in cellular lipids, the cells were incubated for 1 h with [^{3}H]-oleate, and the distribution of radiolabel between lipid classes was then quantified following thin-layer chromatography (TLC) separation. In the control cells, labelling was found predominantly in phospholipids (0.53±0.06 – data are expressed as the proportion of total counts detected) and triglycerides (0.44±0.06), with smaller amounts in diacylglycerol (DAG), monoacylglycerol (MAG) and cholesterol ester (Fig. 1G). In cells that had been starved for 16 h, a greater proportion of the label was incorporated into the phospholipid fraction (0.91±0.01). These proportions returned towards those of the control following a 2 h exposure to 100 μM oleate (phospholipid, 0.72±0.05; triglyceride, 0.26±0.05), demonstrating an increase in the incorporation of oleate into neutral lipids. In cells exposed to 100 μM oleate for 15 min, there was minimal stimulated incorporation of radiolabel into the triglyceride and cholesterol ester fractions, despite the increase in lipid droplets at this time (Fig. 1); nevertheless, there was a small increase in fatty acid (0.06±0.01) and DAG (0.02±0.03) suggesting an increase in lipid biosynthesis.

Lipidomic mass spectrometric analysis of the control cells, starved cells and cells that had been starved followed by treatment with oleate for 15 min demonstrated that there was minimal change in cellular oleate content. There was also no detectable oleate-containing monoglyceride pool (data not shown). The lipidomic analysis confirmed the LD540 experiments in showing an increase in DAG, triglyceride and cholesterol ester content in response to oleate stimulation of starved cells. Analysis of the molecular species demonstrated that a 15 min oleate stimulation of the serum-starved cells particularly elevated 36:2 and, to a lesser extent, 34:2, 34:1 and 36:3 DAG species and 18:1 cholesterol ester (total acyl carbon:total double bonds). The triglyceride species 48:3, 48:2, 50:4, 50:3, 50:2, 52:3, 52:2, 54:3 and 54:2 were particularly elevated, pointing to selective acylation of DAG species (Fig. 2). Because low incorporation of [^{3}H]-oleate into DAG, triglyceride and cholesterol ester was detected (Fig. 1F), this further suggests that stimulated lipid metabolism and/or remodelling underlies the acute generation of lipid droplets. To determine whether oleate stimulated rapid incorporation of fatty acids into the lipids of the lipid drops, serum-starved cells were loaded with the C17 heptadecanoate fatty acid for 2 h prior to stimulation with oleate. Mass spectrometric analysis showed that, at 15 min, the total and the C17 phosphatidic acid levels had decreased, implying

Journal of Cell Science (2014) 127, 3104–3115 doi:10.1242/jcs.145854

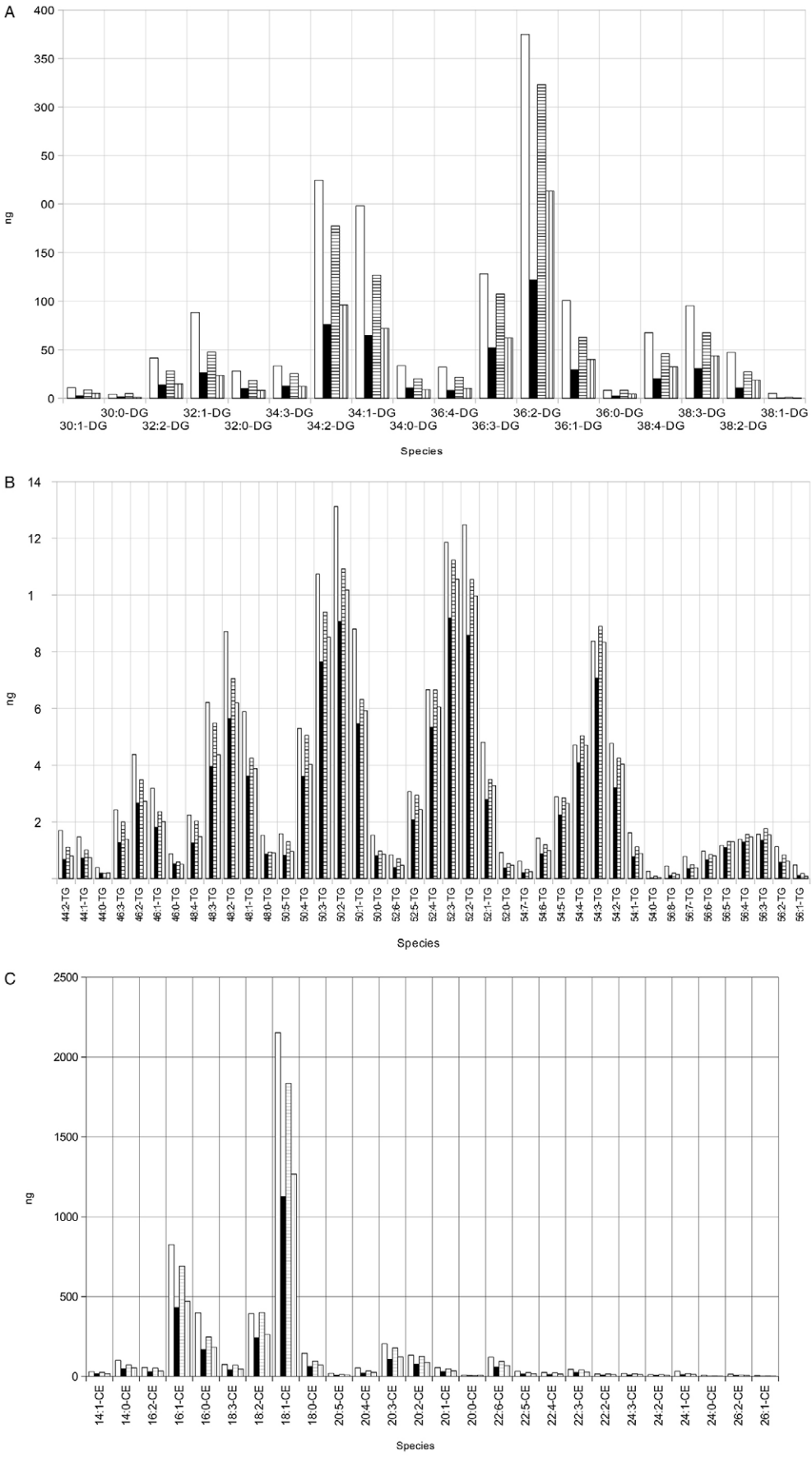

Fig. 2. Mass spectrometric analysis of neutral lipids. Cells were isolated, defined lipid standards were added, and the lipids were extracted using the Folch method. Mass spectrometric determination of individual molecular lipid species was carried out as described in Materials and Methods following HPLC-mediated separation of lipid classes. (A) Diacylglycerol (DG), (B) triglyceride (TG), (C) cholesterol ester (CE). The data are means of duplicate measurements. Open bars, control cells; filled bars, starved cells; horizontal-striped bars, starved cells plus 100 μM oleate for 15 min; vertical-striped bars, starved cells plus 100 μM oleate for 15 min in the presence of 10 μM LY294002 (PI3-kinase inhibitor).

Journal of Cell Science (2014) 127, 3104–3115 doi:10.1242/jcs.145854

Table 1 Mass spectrometric measurement of lipids in heptadecanoate-loaded cells

Quantification of lipid species in a particular lipid class that contain a C-17-fatty-acyl-derived group				
C-17 lipid ($\times 10^6$ ng)	0-min oleate	15-min oleate	30-min oleate	120-min oleate
MAG	1.8	1.63	0.99	0.25
DAG	170	180	170	201
TG	8600	8245	8310	8385
PA	44	21	17	14
CE	14	13	8	3
FACoA	0.12	0.13	0.13	0.1
PC	2060	2390	2082	2331
Quantification of all lipids present in a particular lipid class				
Lipid ($\times 10^6$ ng)	0-min oleate	15-min oleate	30-min oleate	120-min oleate
MAG	29.5	135.5	117	154
DAG	2771	3502	3494	4010
TG	11,805	10,895	11,545	15,428
PA	734	494	471	379
CE	271	211	210	110
FACoA	12.5	13.9	13.5	13.2
PC	45,905	51,005	44,845	52,100

Cells were incubated for 18 h in DMEM+1% BSA, followed by the addition of 3 μM heptadecanoate. Following a further 2 h, the cells were stimulated with 100 μM oleate. The lipids were extracted at the times indicated and quantified by mass spectrometry. The data are means of duplicate measurements from a single experiment. MAG, monoacylglycerol; DAG, diacylglycerol; TG, triglyceride; PA, phosphatidic acid; CE, cholesterol ester; FACoA, fatty acylCoA; PC, phosphatidylcholine.

increased *de novo* triglyceride synthesis. The extremely high amounts of triglyceride relative to other lipids makes it impossible to quantify the shift in lipids from MAG, DAG and phosphatidic acid to triglyceride (see Table 1). Additionally, total MAG and DAG increased after 15 min but there was no increase in C17 incorporation – the level of C17 cholesterol ester declined as oleate incorporation was increased. These data support the proposition that at the early (up to 15 min) time-points the increase in lipids in droplets comes from increased synthesis from existing cellular lipids, rather than the incorporation of external oleate.

In cells that were stimulated by the addition of medium containing 100 μM oleate for 10 min, after which the oleate was removed and the cells were washed with warmed PBS,

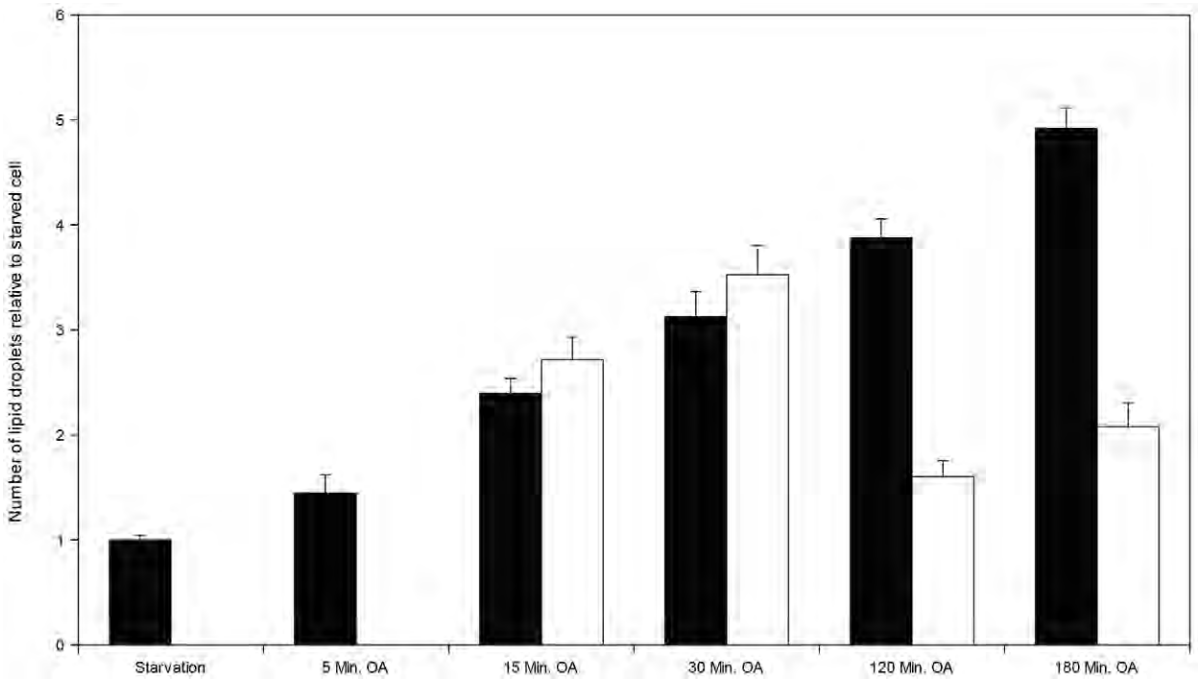

Fig. 3. Dependence of continued lipid droplet formation upon extracellular oleate. Starved Huh-7 cells were exposed to 100 μM oleate (OA) for 10 min. Subsequently, either this was maintained (black bars) or the medium was removed and, following a PBS wash, the cells were incubated in fresh fatty-acid-free medium (open bars). The cells were fixed at the stated time-points, and lipid droplets were identified by LD540 staining and quantified by using microscopy. The data were normalised to results from fatty-acid-starved cells (starvation) and are expressed as the mean±s.e.m. The *P*-values are: 15 min, $P=0.9$; 30 min, $P=0.5$; 120 min, $P<10^{-10}$; 180 min $P<10^{-10}$ (Student's *t*-test).

Journal of Cell Science (2014) 127, 3104–3115 doi:10.1242/jcs.145854

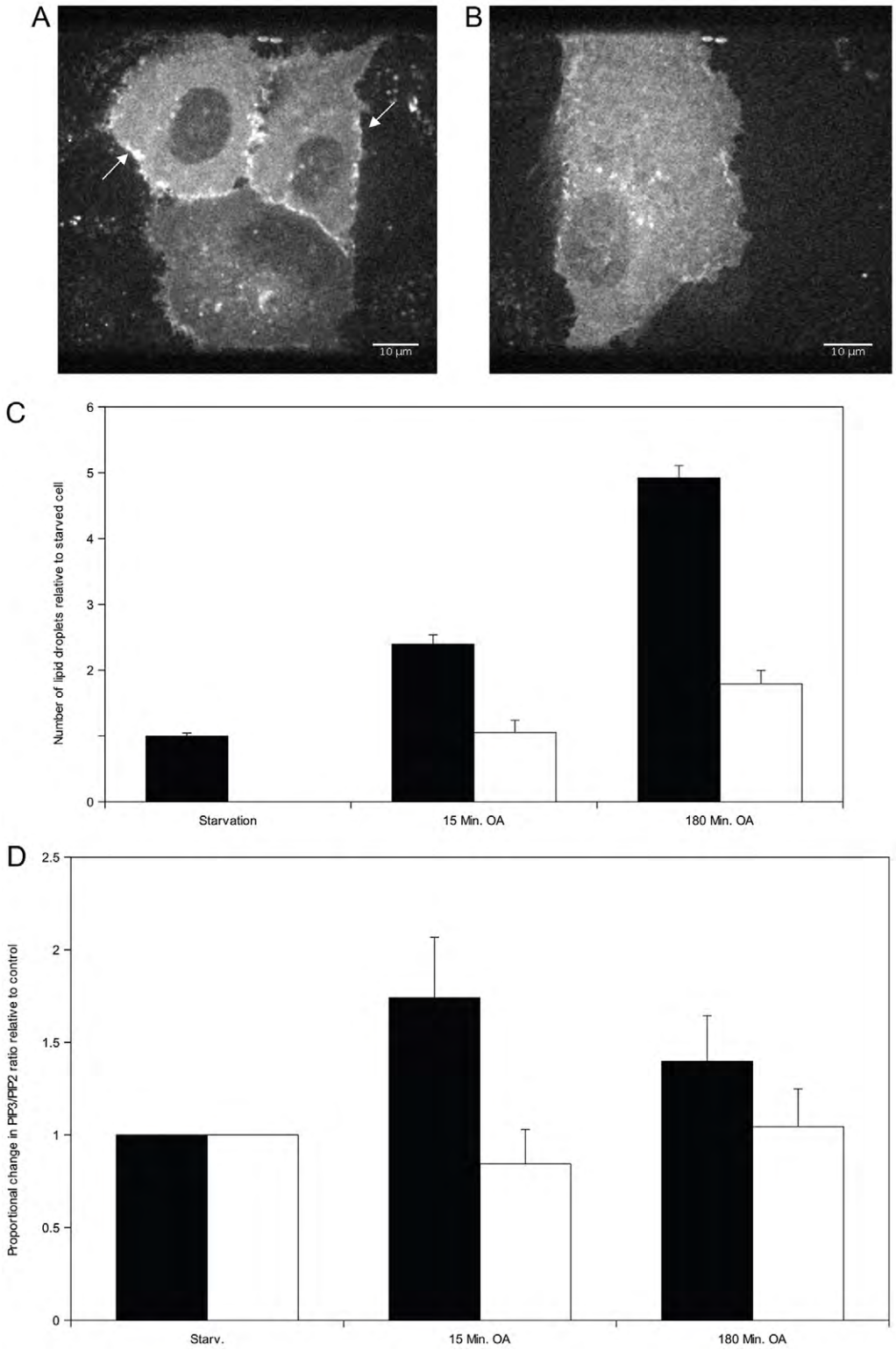

Fig. 4. Regulation of lipid droplet formation by PI3-kinase activity. The localisation of EGFP–Grp1-PH was examined by spinning disk confocal recording of cells stably expressing the fusion protein. (A) Translocation of EGFP–Grp1-PH to the plasma membrane was observed following stimulation with oleate for 1 min (arrows). (B) No GPR1–EGFP translocation to the plasma membrane was observed following stimulation with the short-chain capric acid. (C) Huh-7 cells were preincubated with the PI3-kinase inhibitor LY294002 (10 μM) prior to stimulation with 100 μM oleate (OA) for 15 min or 180 min. Open bars, LY294002-treated cells; closed bars, untreated cells. Data are expressed as the mean±s.e.m., normalised to the number of lipid droplets in fatty-acid-starved cells (starvation). The *P*-values are: 15 min, $P=0.005$; 180 min, $P<0.001$ (Student's *t*-test). (D) The ratio of PtdIns(3,4,5)P_3:PtdInsP_2 in Huh-7 cells after stimulation with 100 μM oleate. The data were normalised to results from fatty-acid-starved cells (Starv) and are expressed as the mean±s.d. The *P*-values are: 15 min, $P=0.2$; 180 min, $P=0.09$ (Mann-Whitney U test). Closed bars, control Huh-7 cells; open bars, FFAR4-knockdown cells (see Fig. 8).

lipid droplet formation continued, as though the oleate had remained present, for at least a further 20 min (Fig. 3). The fold increase in the number of lipid droplets above that of the starved control cells after 30 min (i.e. 10 min oleate exposure followed by 20 min in its absence) was 3.52±0.28, but this declined to 1.6±0.16-fold after 2 h, which was similar to the fold change in lipid droplet number observed after a 5 min oleate stimulation (1.45±0.17).

An increase in lipid droplet generation was also observed in starved cells in response to the addition of other long-chain fatty acids (e.g. linoleic acid), but not short-chain fatty acids (e.g. capric acid) (data not shown), further indicating the involvement of a fatty-acid-stimulated signalling pathway. A number of signalling pathways have been proposed to be important for lipid droplet formation. Fig. 4 demonstrates that the phosphoinositide 3-kinase (PI3-kinase) pathway is crucial for lipid droplet generation in

Journal of Cell Science (2014) 127, 3104–3115 doi:10.1242/jcs.145854

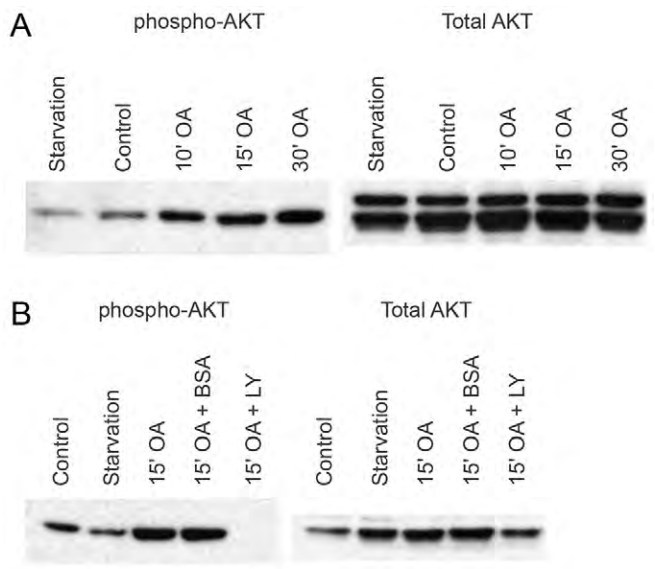

Fig. 5. Phosphorylation of AKT in oleate-stimulated cells. (A) Cells were treated with 100 μM oleate (OA) and cell extracts were subjected to SDS-PAGE and western blotting for AKT and phosphorylated (phospho)-AKT. (B) Western blotting as above using cells that were incubated with the PI3-kinase inhibitor LY294002 (LY) prior to stimulation with 100 μM oleate. The presence of 1% BSA during stimulation with oleate did not alter the response.

oleate-stimulated starved cells. Preincubation with 10 μM LY294002 (a PI3-kinase inhibitor) prior to oleate stimulation completely inhibited lipid droplet generation at the 15 min time-point and significantly suppressed the fold increase in lipid droplet number at 180 min (control, 5.10±0.19; +LY294002, 1.79±0.21) (Fig. 4C). Mass spectrometric analysis also showed that the oleate-stimulated increases in DAG, triglyceride and cholesterol ester species were inhibited by LY294002 (Fig. 2). This indicates a strong dependence of droplet generation upon PI3-kinase-dependent signalling. To confirm the involvement of PI3-kinase signalling in oleate stimulation, three strategies were adopted. First, measurement of phosphatidylinositol (3,4,5)-trisphosphate [PtdIns(3,4,5)P_3] concentration by mass spectrometry demonstrated an oleate-stimulated increase in cellular PtdIns(3,4,5)P_3, as quantified by the PtdIns(3,4,5)P_3:PtdInsP_2 (phosphatidylinositol 4,5-bisphosphate) ratio (see Fig. 4D). Additional mass spectrometric analysis demonstrated that the increased PtdIns(3,4,5)P_3 was either the 38:4 or 38:3 species (not shown). Second, western blotting showed that oleate stimulated the phosphorylation of AKT (also known as protein kinase B). This was detectable by 10 min (Fig. 5A) and continued to 30 min, but was inhibited in cells that were preincubated with 10 μM LY294002 (Fig. 5B). Third, we used Huh-7 cells stably expressing a PtdIns(3,4,5)P_3-binding GRP1-PH domain tagged with GFP to show that oleate stimulated the translocation of the PH domain to the plasma membrane (Fig. 4A). By contrast, 100 μM capric acid, which did not induce lipid droplet formation, was not able to induce plasma membrane translocation (Fig. 4B). Examination of the localisation of the Grp1-PH domain also demonstrated that there was no colocalisation, in either control or oleate-stimulated cells, between the PtdIns(3,4,5)P_3-binding domain and the lipid droplets.

Previous reports have suggested that PLD and ERK signalling play a role in lipid droplet formation (Nakamura et al., 2005, Andersson et al., 2006). However, incubation of Huh-7 cells with oleate failed to increase the phosphorylation of ERK (data not shown), and the inclusion of the ERK inhibitor (10 μM PD98059) failed to affect oleate-stimulated lipid droplet formation. By contrast, droplet generation was found to be dependent upon both PLD1 and PLD2 activities. Preincubation with either 100 nM PLD1 or PLD2 inhibitor (Scott et al., 2009) prevented lipid droplet formation in response to oleate stimulation (Fig. 6D). In cells stimulated with oleate for 15 min, inhibition of either PLD isoform was equally effective (fold change in lipid droplet number following PLD1 inhibition, 1.06±0.19; PLD2 inhibition, 1.26±0.31; untreated, 3.12±0.24); whereas, after 180 min, inhibition of PLD1 but not PLD1 was effective in inhibiting lipid droplet formation (PLD1 inhibitor, 3.19±0.21; untreated, 5.1±0.19; PLD2 inhibitor, 4.23±0.68).

Examining Huh-7 cells stably expressing pEGFP-PLD1 and co-stained with LD540 for lipid droplet detection (Fig. 6A–D) demonstrated extensive but not exclusive colocalization of PLD1 with lipid droplets, suggesting that PLD1 is involved in lipid droplet processing. PLD1 also colocalised with ARF1, one of the small GTPases known to regulate the activity of the phospholipase (Fig. 6E). These data suggest that oleate stimulates a receptor-activated signalling pathway in Huh-7 cells that leads to an increase in lipid droplet formation. Further evidence for this proposition was provided by incubating cells overnight with pertussis toxin, which inhibited oleate-stimulated lipid droplet formation, thereby implicating a Gi/Go-coupled receptor in this pathway (Fig. 1F). GW9508, an agonist of the long-chain fatty acid receptor, primarily active upon FFAR1 and FFAR4, induced lipid droplet formation in Huh-7 cells in the absence of exogenous fatty acids (Fig. 7A). This was apparent after 15 min, when the fold increase in droplet formation was similar to that induced by oleate (oleate, 2.69±0.14; GW9508, 2.88±0.72); however, in contrast to oleate, a longer stimulation (180 min) did not further increase lipid droplet number (oleate, 5.1±0.19; GW9508, 2.71±0.89). In parallel with the increase in lipid droplet formation, GW9508 induced the phosphorylation of AKT (Fig. 7B).

Western blotting of membrane preparations from Huh-7 cells demonstrated the presence of the FFAR4 but not FFAR1 fatty acid receptor, pointing to the former as the receptor responsible for oleate-stimulated lipid droplet formation (Fig. 8A). FFAR4 was also detectable in HeLa cells but not in HEK293 cells (Fig. 8A). To determine the importance of FFAR4 in regulating oleate-stimulated lipid droplet formation, a stable pLKO-vector-based cell line expressing FFAR4 shRNA was established, along with an empty-vector-containing Huh-7 cell line to be used as a control. Western blotting demonstrated that the shRNA suppressed the expression of FFAR4 (Fig. 8A). Quantification of lipid droplets in the FFAR4-knockdown cell line compared with droplet numbers from the pLKO control cell line showed a reduction in response to both a 15 min (Fig. 8B) (pLKO, 2.37±0.41; FFAR4-knockdown, 1.37±0.14) and a 180 min oleate stimulation (pLKO, 7.18±1.02; FFAR4-knockdown, 3.64±0.34). The inhibitory effect of the shRNA could be reversed by transiently transfecting the cells with FFAR4-pEGFP (15 min, 2.26±0.35; 180 min, 5.64±0.58) but not with the functionally disabled construct FFAR4RH-pEGFP (15 min, 0.76±0.17; 180 min, 3.08±0.31). In parallel with the reduction in lipid droplet formation, western blotting of oleate-stimulated FFAR4-knockdown cells demonstrated reduced AKT phosphorylation compared with that of cells transiently transfected with FFAR4-pEGFP (Fig. 8C,D); this was apparent primarily at 15 min. To further characterise the signalling pathways linked to oleate activation of FFAR4, changes in the PtdIns(3,4,5)P_3:PtdInsP_2

Journal of Cell Science (2014) 127, 3104–3115 doi:10.1242/jcs.145854

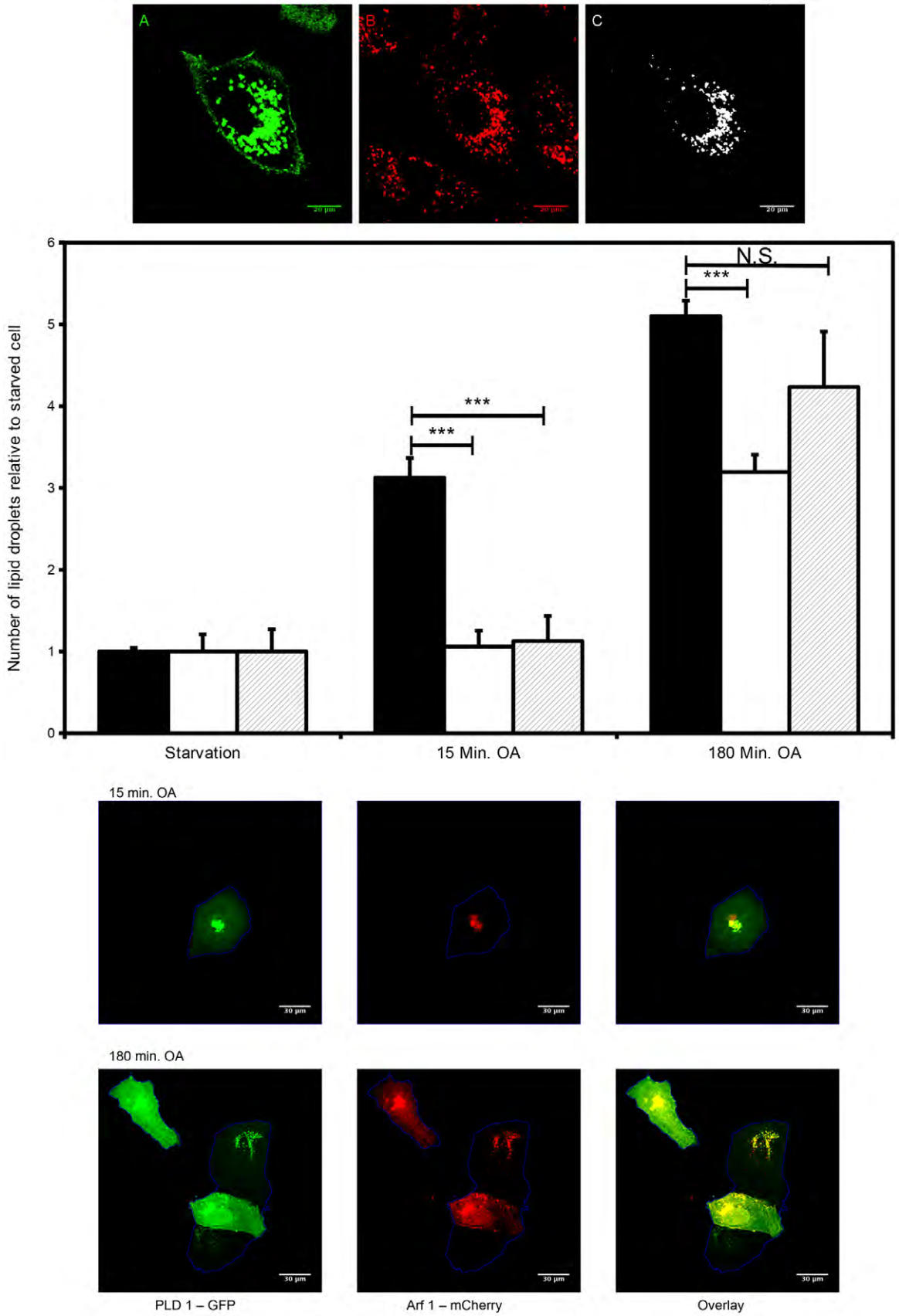

Fig. 6. See next page for legend.

Journal of Cell Science (2014) 127, 3104–3115 doi:10.1242/jcs.145854

Fig. 6. PLD partially colocalises with lipid droplets in Huh-7-cells and is necessary for lipid droplet formation. Huh-7 cells expressing GFP–PLD1 (A, green) and stained with LD540 (B, red). The isolated colocalised pixels from GFP–PLD1 and LD540 images was determined using ImageJ – the RGB colocalisation plugin showed a strong association of PLD1 with lipid droplets (C, white). (D) Preincubation of Huh-7 cells with the PLD1 or PLD2 inhibitors (each at 100 nM) prior to stimulation with 100 μM oleate (OA). Closed bars, control cells; open bars, PLD1 inhibitor; horizontal-striped bars, PLD2 inhibitor. The data were normalised to the number of lipid droplets in fatty-acid-starved cells (starvation) and are expressed as the mean±s.e.m. The *P*-values are: 15 min PLD1 inhibitor, $P=9.4\times10^{-5}$; 15 min PLD2 inhibitor, $P=0.0002$; 180 min PLD1 inhibitor, $P=1\times10^{-8}$; 180 min PLD2 inhibitor, $P=0.09$ (Student's *t*-test). N.S, non-significant. (E) Maximum projection of 3D confocal recordings of transiently transfected Huh-7 cells. Cells were transfected with GFP–PLD1 (green, left) and Arf1–mCherry (red, middle). Cells were stimulated for 15 min or 180 min with 100 μM oleate prior to fixing and imaging. Some colocalisation (yellow) was observed in control starved cells (not shown).

ratio were determined by mass spectrometry in FFAR4-knockdown cells compared with the changes in pLKO-expressing cells (Fig. 4D). A 1.74±0.32-fold stimulation in response to oleate stimulation for 15 min was detected in the pLKO cells, but this was not observed in the FFAR4-knockdown cells (0.84±0.19).

Not only could transfection of FFAR4-pEGP rescue the oleate stimulation of lipid droplet formation in FFAR4-knockdown cells, but the alterative receptor FFAR1 could also substitute for FFAR4. Stimulation of the FFAR1-transfected cells with 100 μM oleate generated a similar increase in the number of lipid droplets as was observed in mock-transfected pLKO cells, and this recovered response was ablated by preincubation with LY294002 (data not shown), indicating that the same signalling pathway is used by both fatty acid receptors.

DISCUSSION

The accumulation of excess lipid in cells and tissues has been associated with pathological disorders, such as insulin resistance and even heart failure. It is thus essential that cells store lipids in a highly regulated manner in lipid droplets. However, lipid droplets are more than simple storage structures; instead, they are specialised dynamic organelles that can also operate as a platform for intracellular signalling and viral synthesis. Thus, their regulation is crucial, and it is surprising that little is known about the acute regulation of their formation. Lipid droplet formation clearly requires cellular lipid uptake, modification and subsequent storage in the organelle (Sturley and Hussain, 2012; Brasaemle and Wolins, 2012); nevertheless, the results presented in this paper point to a regulated process of lipid droplet generation, rather than it being solely a consequence of increased lipid uptake.

The dynamic nature of cellular lipid droplets is demonstrated by their reduction in response to starvation and the subsequent recovery in number following the addition of exogenous fatty acids, notably oleate (Fig. 1). It is not possible to state whether the droplets are lost in response to starvation or whether they become too small to be detectable or become lipid-free structures that cannot be detected using lipid-specific dyes such as LD540. However, it is clear that the addition of oleate to serum-free medium rapidly induces the appearance of detectable lipid droplets. The [^{3}H]-oleate incorporation experiments (Fig. 1G) and C-17 fatty acid mass spectrometry experiments (Table 1) demonstrated that at short times (15 and 30 min) following oleate addition to the medium there was limited incorporation of fatty acid into triglycerides and cholesterol ester, despite there being a significant increase in the number and size of lipid droplets (see Fig. 1A–C). This implies that oleate addition stimulates the incorporation of endogenous cellular lipid into lipid droplets, as demonstrated by the mass spectrometric analysis (Table 1; Fig. 2), with the non-regular increase in lipid droplet size either being due to stimulated droplet fusion or variable increases in uptake into particular droplets. By contrast, the longer incubation with oleate demonstrates a clearer incorporation of added [^{3}H]-oleate into droplet-associated lipids and also a significant increase in total triglyceride content.

This clearly biphasic generation of lipid droplets in response to oleate points to distinct mechanisms of their formation. Whereas the longer-time-dependent increase is undoubtedly dependent upon oleate uptake and incorporation, the more acute response is suggestive of a signalling process. This is supported by the data presented in Figs 2, 3 and 7, which show that a pulse of oleate can stimulate lipid droplet formation, that the droplet formation is specific for long-chain monounsaturated lipids and that GW9508, a small molecule agonist of the FFAR1 and FFAR4 fatty acid receptors, can replace oleate in stimulating the short-term but not the long-term increase in lipid droplet formation. The Huh-7 cells examined in this study express FFAR4, but not FFAR1, pointing to the role of these receptors in oleate-stimulated lipid droplet formation; indeed, depletion of the FFAR4, using an shRNA approach, ablated oleate-stimulated droplet formation following a 15 min incubation and significantly suppressed droplet formation after 120 min (Fig. 8).

Occupation of the FFAR4 fatty acid receptor stimulates lipid droplet formation through a signalling cascade. It has been previously suggested that lipid droplet formation requires PLD and ERK activity (Andersson et al., 2006). Although our inhibitor studies provide support for the proposal that PLD activity plays a role in droplet formation, with apparent differences in the functions of PLD1 and PLD2, we found no evidence for ERK involvement; it is possible that this difference in result is due to our use of a newer generation of more specific ERK inhibitors. In addition to PLD signalling, ligating the FFAR4 receptor activates PI3-kinase, presumably through the pertussis-toxin-sensitive Gi. This is detectable as an increase in PtdIns(3,4,5)P_3 mass, as measured by mass spectrometry, in response to oleate stimulation in control but not FFAR4-knockdown cells and by an increase in oleate-stimulated AKT phosphorylation, which was sensitive to the PI3-kinase inhibitor LY294002 and could be mimicked by GW9508. In addition, we observed an increase in the plasma membrane localisation of a transfected GFP–Grp1-PH-domain in response to oleate but not capric acid stimulation, and we did not detect accumulation of PtdIns(3,4,5)P_3 at the lipid droplet. The localisation of PtdIns(3,4,5)P_3 at the plasma membrane implies that this is the receptor-linked signalling process that stimulates lipid droplet formation. PLD, by contrast, appears to be more closely associated with the droplet, along with its regulatory small GTPase, ARF1. This suggests that PLD signalling is downstream of PI3-kinase in the oleate-stimulated cascade, and that it might have a more direct effect upon the lipid droplet. Both PLD1 and PLD2 inhibitors have an inhibitory effect upon acute oleate-stimulated lipid droplet formation; by contrast, longer term droplet formation is also inhibited by the inhibition of PLD1, whereas the inhibition of PLD2 has a minimal effect. PLD2 is a plasma-membrane-localised isoform (McDermott et al., 2004), thus pointing to PLD1 as a major regulator at the lipid droplet. The stimulation of PLD activity by oleate acting through a fatty

Journal of Cell Science (2014) 127, 3104–3115 doi:10.1242/jcs.145854

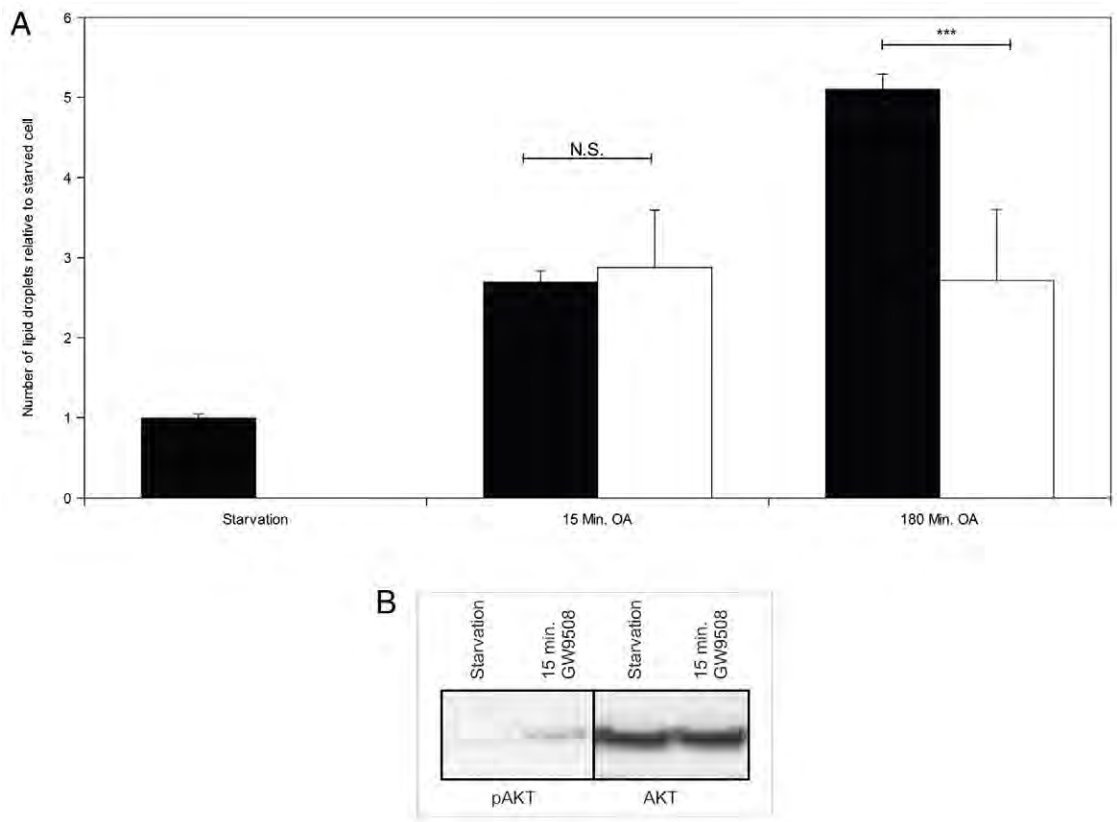

Fig. 7. Stimulation of cells with FFAR4 agonist. (A) Quantification of lipid droplets from 3D confocal recordings in cells stimulated with the FFAR4 agonist GW9508 (open bars) compared with control cells (closed bars) after oleate (OA) stimulation. The data were normalised to results from fatty-acid-starved cells (starvation) and are expressed as the mean±s.e.m. The *P*-values are: 15 min, $P=0.8$; 180 min, $P=0.0003$ (Student's *t*-test). N.S., non-significant. (B) Western blots to show AKT phosphorylation (pAKT) in the GW9508-stimulated cells.

acid receptor also provides an explanation for the long-standing issue that there is an oleate-stimulated PLD enzyme (Kasai et al., 1998) in cells that has never been identified – receptor-mediated stimulation of PLD1 and PLD2 following oleate treatment thus removes the need to implicate an unidentified PLD species.

The recognised role of PLD in regulating membrane trafficking, fusion and fission events suggests that this enzyme might be directly involved in oleate-stimulated lipid droplet formation, whether this happens using existing droplets, by budding from the endoplasmic reticulum (Robenek et al., 2009) or fission of lipid droplets (Long et al., 2012) remains to be resolved. How PI3-kinase regulates the process is unclear, although the fact that its inhibition ablates the increase in droplet number both after 15 min and 180 min exposure to oleate implies a fundamental regulatory role. Although PtdIns(3,4,5)P_3 can regulate guanine nucleotide exchange factors (GEFs) such as Arno (officially known as CYTH2) that activate ARF and thereby control PLD1 activity, there might be a separate function for AKT signalling that remains to be determined. A role for PI3-kinase signalling in regulating lipid droplets has been previously suggested. In microglia, the generation of lipid droplets following lipopolysaccharide (LPS) stimulation is sensitive to LY294002 (Khatchadourian et al., 2012). A regulatory effect of AKT upon the lipid droplet pool in different cell types through insulin signalling has also been suggested (Vereshchagina and Wilson, 2006; Bell et al., 2008). Inhibition of PLD activity only fully ablates oleate-stimulated droplet formation at early time-points, linking it to the receptor-stimulated pathway. At later time-points there is only partial inhibition, suggesting either that other phosphatidic-acid-generating pathways can compensate at these times, or that only the early stimulated pathway is phosphatidic-acid-dependent, provided that the molecular species is similar to that generated by PLD (Pettitt et al., 2001). This is in contrast to PI3-kinase activity, which appears to be fully essential for lipid droplet formation. An additional possibility is suggested by the reports that phosphatidic acid can regulate mTOR (Fang et al., 2001), although this has proved to be a contentious suggestion. Nevertheless, if both PLD and PI3-kinase activities are feeding into an increase in mTOR activity this might be a means to activate lipid droplet formation – indeed, mTOR is known to promote cellular lipid storage.

The data in this paper suggest a model in which the length of exposure to elevated concentrations of fatty acid is crucial for the mechanism of lipid droplet formation; short-term exposure stimulates the generation or growth of droplets in cells primarily from endogenous lipid, whereas longer exposure results in the incorporation of exogenous lipid following uptake. This could suggest that the magnitude and length of exposure to elevated concentrations of fatty acids could be an important switch in regulating the amount of lipid droplet formation and, thus, between health and disease. In healthy states, the lipid droplets serve as storage devices for lipids, whereas, in diseases, such as obesity and type 2 diabetes, excess droplet formation occurs. PI3-kinase inhibitors have been considered as anti-insulin drugs, and they might also prove to be effective in reducing lipid deposition. Alternatively, PLD inhibitors could play a role in reducing acute lipid droplet formation in response to a high-fat diet. The effects of FFAR4 dysfunction have been demonstrated by Ichimura et al., using a combined epidemiological and knockout approach (Ichimura et al., 2012). The importance of a functioning FFAR4 receptor was shown – in its absence there was an increase in obesity, including a fatty liver. This points to a key regulatory role for the signalling pathway activated by this receptor, in contrast to the more deleterious effects observed following unregulated lipid uptake in its absence.

Journal of Cell Science (2014) 127, 3104–3115 doi:10.1242/jcs.145854

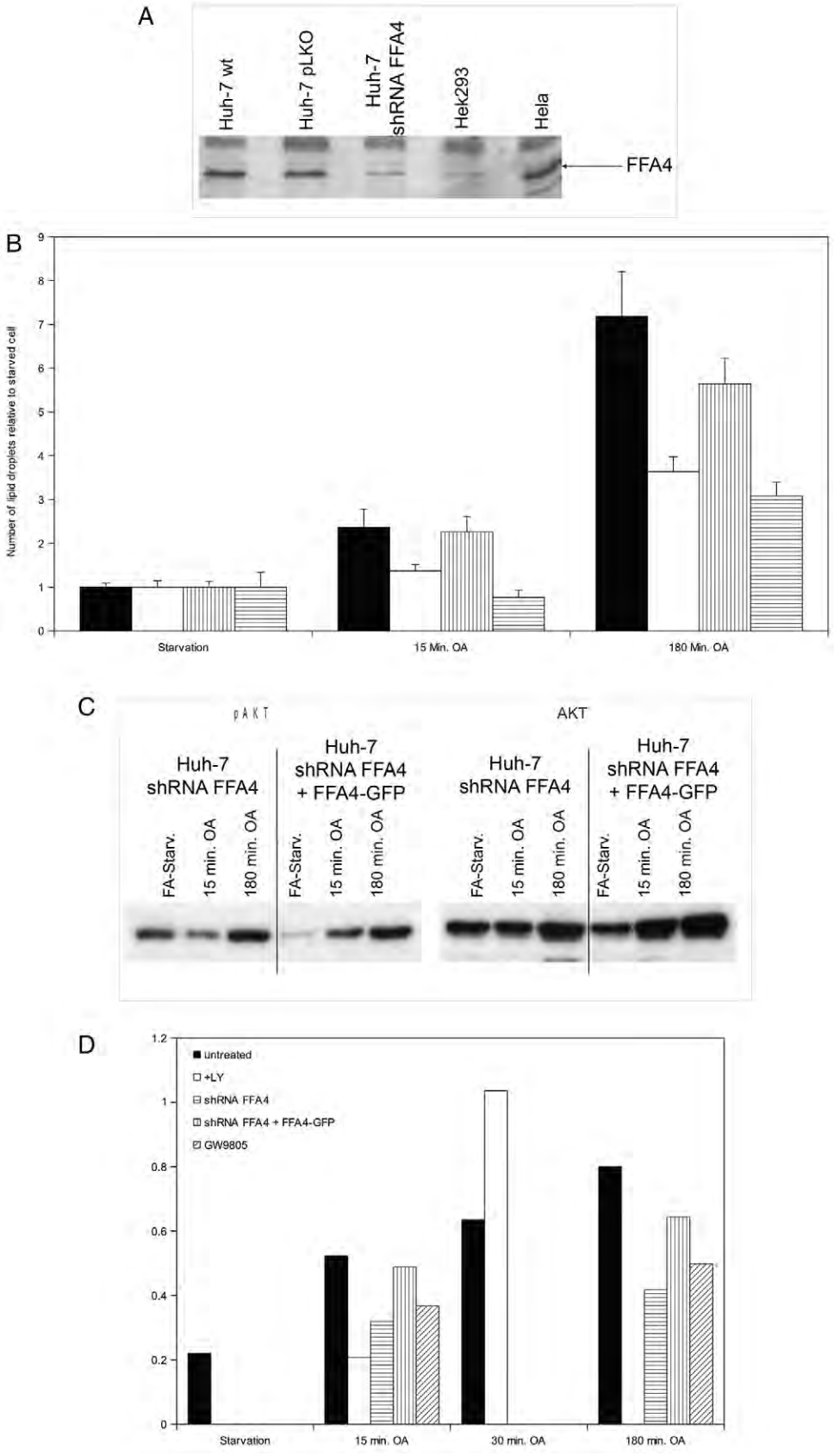

Fig. 8. The long-chain fatty acid receptor FFAR4 mediates oleate-stimulated signalling. (A) Detection of FFAR4 (FFA4) in Huh-7 cells and Hela cells. wt, wild type. (B) The effects of knockdown of FFAR4 in Huh-7 cells. Open bars, Huh-7 cells stably expressing FFAR4 shRNA; closed bars, cells transfected with an empty pLKO vector; vertical-striped bars, additional transfection with FFAR4–GFP; horizontal-striped bars, additional transfection with a non-functional dominant-negative mutant (FFAR4RH). OA, oleate. Data are expressed as the mean±s.e.m. The *P*-values are: 15 min FFAR4 shRNA knockdown, $P=0.014$; 15 min FFAR4 shRNA knockdown+FFAR4–GFP, $P=0.093$; 180 min FFAR4 shRNA knockdown, $P=0.375$; 180 min FFAR4 shRNA knockdown+FFAR4–GFP, $P=0.531$; 15 min FFAR4 shRNA knockdown+FFAR4RH, $P=0.078$; 180 min FFAR4 shRNA knockdown+FFAR4RH, $P=0.391$ (Mann-Whitney U test). (C) Phosphorylation of AKT in the shRNA-treated cells. FA-Starv, fatty-acid-starved cells. (D) Relative quantification of the data from multiple blots determining changes in AKT phosphorylation (representative blot shown in Fig. 8C). LY, PI3-kinase inhibitor LY294002.

Journal of Cell Science (2014) 127, 3104–3115 doi:10.1242/jcs.145854

MATERIALS AND METHODS

Cell culture and stimulation

Huh-7 cells were grown to a confluency of 50% in DMEM (PAA) supplemented with 10% fetal calf serum (FCS) (PAA) and 1% penicillin-streptomycin on 22-mm round coverslips (VWR). The medium was replaced with DMEM supplemented with 1% penicillin-streptomycin and 1% bovine serum albumin (BSA; fatty acid free, endotoxin free) for starvation for 16 h prior to stimulation with fatty acids, agonists or inhibitors. The PLD1 and PLD2 inhibitors were used as described previously (Norton et al., 2011). LY294002 (Calbiochem) in DMSO was applied 20 min before stimulation at a final concentration of 10 µM.

Confocal microscopy

Cells were fixed by incubating with 800 µl of 4% paraformaldehyde (PFA) in PBS for 45 min at room temperature and then washing three times with 1 ml of ice-cold PBS. Samples were stained with 800 µl of LD540 (diluted 1:1000 in PBS; provided by Christophe Thiele, Bonn, Germany) and Hoechst 33342 (1:10,000) for 10 min. The cells were viewed under 1 ml of PBS during recording using an Olympus FLUOVIEW FV1000 at a resolution of 0.265 µm/pixel, 800×800 pixel. The *z* dimensions were 25×0.45 µm/slice. The excitation wavelengths were 405 nm for Hoechst 33342 and 488 nm for LD540, and the filter settings for recording were SDM490, 425–420 nm for Hoechst 33342; 500–600 nm for LD540. Three-dimensional (3D) quantification of lipid droplets was performed with Volocity® 3D Image Analysis Software (PerkinElmer). For live-cell imaging of GPR1–GFP-transfected Huh7-cells, a spinning disc confocal microscope was used with filter settings for GFP (excitation 488 nm, emission ≥525nm). The exposure time was 350 ms.

Western blotting

SDS-PAGE was performed using 10% acrylamide gels with kaleidoscope pre-stained standards. Semi-dry transfer preceded blotting with the following primary antibodies: rabbit anti-AKT, anti-phospho-AKT (Cell Signaling Technologies), rabbit anti-FFAR4 (MBL) and rabbit anti-FFAR1 (Abcam). Incubation with the secondary antibody (HRP-coupled anti-rabbit-IgG) was followed by ECL detection using Hyperfilm ECL high performance chemiluminescence film (Amersham).

Lipid analysis

After stimulation, PtdIns(3,4,5)P_3 was determined by mass spectrometry as described previously (Clark et al., 2011), and neutral lipids were determined by mass spectrometry as described previously (Griffiths et al., 2013; Gaunt et al., 2013). Huh-7 cells were incubated with 1 µCi of [^{3}H]-oleic acid in DMEM containing 1% penicillin-streptomycin and 1% fatty-acid-free BSA for 1 h prior to stimulation. Lipids were extracted from cell pellets using the Folch method. A total of 1 µg of TLC Mix 40 (Larodan) was added as a standard, and lipids were separated by TLC on activated silica gel 60 (Merck) plates developed using hexane:diethylether:acetic acid (80:20:1). Lipids were identified with iodine vapour, scraped from the plate and the radioactivity was determined by scintillation counting. Huh-7 cells were loaded with 3 µM C17 heptadecanoate fatty acid in DMEM containing 1% penicillin-streptomycin and 1% fatty-acid-free BSA for 2 h before oleate stimulation.

Mass spectrometry

Cell pellets (6×10^6 cells) were washed twice with cold PBS and resuspended in 1.5 ml of methanol in silanised glass tubes on dry ice. After spiking with 400 ng of 17:0/20:4-phosphatidylinositol, 400 ng of 12:0/12:0-phosphatidylcholine, 100 ng of 12:0/12:0-phosphatidic acid, 100 ng of 12:0/12:012:0-triglyceride, 100 ng of 12:0/12:0-DAG, 50 ng of 12:0-MAG, 200 ng of 17:0-free fatty acid, 100 ng of d7-cholesterol and 100 ng of 17:0-cholesterol ester as internal standards, 1.5 ml of 0.88% NaCl and 3 ml of chloroform were added. The mixture was vortexed for 20 s at room temperature and sonicated in an ice-cold sonication water bath for 2 min, and then centrifuged at 1000 ***g*** at 4℃ for 15 min. The lower phase was collected. The upper phase was extracted with 3 ml of synthetic lower phase and the resulting extractions were combined and dried under vacuum at room temperature with SpeedVac (Thermo) and redissolved in 100 µl of chloroform. A total of 7 µl was injected for liquid chromatography-mass spectrometry (LC/MS) analysis. For LC/MS analysis, we used a Thermo Orbitrap Elite system (Thermo Fisher) hyphenated with a five-channel online degasser, four-pump, column oven and autosampler with cooler, Shimadzu Prominence HPLC system (Shimadzu) for lipids analysis. In detail, lipid classes were separated on a normal phase silica gel column (2.1×150 mm, 4micro, MicoSolv Technology) with a hexane/dichloromethane/chloroform/methanol/acetanitrile/water/ethylamine solvent gradient based on the polarity of head group. High resolution (240 k at m/z 400)/accurate mass (with mass accuracy <5 ppm) and tandem mass spectrometry [collision induced dissociation (CID) fragmentation] were used for molecular species identification and quantification. The identity of lipid was further confirmed by reference to appropriate lipids standards. The Orbitrap Elite mass spectrometer operation conditions for positive-ion lipids analysis were as follows: heated electrospray ionisation (ESI) source in positive ESI mode, heater temperature of 325℃, sheath gas flow rate (arb) of 35, aux gas flow rate (arb) of 5, sweep gas flow rate (arb) of 0, I spray voltage of 3.5 kV, capillary temperature of 325℃, S-lens radio frequency level of 60%. The Orbitrap mass analyser was operated as SIM scan mode with two events. Event 1 – mass range, m/z 238–663; mass resolution, 240 k at m/z 400. Event 2 – mass range, m/z 663–1088; mass resolution, 240 k at m/z 400. The Orbitrap Elite mass spectrometer operation conditions for negative ion lipids analysis were as follows: heated ESI source in negative ESI mode, heater temperature of 325℃, sheath gas flow rate (arb) of 45, aux gas flow rate (arb) of 10, sweep gas flow rate (arb) of 0, I spray voltage of 3.0 kV, capillary temperature of 375C°, S-lens RF level of 70%. The Orbitrap mass analyser was operated as SIM scan mode with two events. Event 1 – mass range, m/z 218–628; mass resolution, 240 k at m/z 400. Event 2 – mass range, m/z 628–1038; mass resolution, 240 k at m/z 400. The ion trap mass analyser was operated as dependent scan in CID mode at normal scan speed. All the solvents used for lipid extraction and LC/MS/MS analysis are LC-MS grade from Fisher Scientific.

For cholesterol and cholesterol ester analysis, the lipid extract was acetylated with 170 µl acetyl chloride:chloroform (1:5) at room temperature for 2 h. Solvent was removed at room temperature under vacuum. The acetylated lipid was re-dissolved in 70 µl of 10 mM ammonium acetate methanol:chloroform (3:1). A total of 7 µl was injected by autosampler for ESI-MS/MS analysis using a Shimadzu Prominence HPLC hyphenated with ABSciex 4000 QTRAP. 0.25 ml/min 10 mM ammonium acetate methanol:chloroform (3:1) was pumped to the 4000 QTRAP source for ESI-MS/MS analysis. The following mass spectrometry operation parameters were used. Source/gas parameters: curtain gas, 20; collision gas, medium; IonSpray voltage, 5500; temperature, 400℃; ion source gas 1, 45; ion source gas 2, 20; interface heater, on. Compound parameters: entrance potential (EP), 9.0; collision cell exit potential (CXP), 11.0; declustering potential, 60 for cholesterol ester analysis and 50 for acetylated cholesterol analysis; collision energy, 19 for cholesterol ester analysis and 15 for acetylated cholesterol analysis. Unit resolution was used for both Q1 Mass and Q3 Mass for multiple reaction monitoring analysis of cholesterol ester and cholesterol.

Transfection and cell line generation

Huh-7 cells were transfected using FuGENE 6 (Roche). For selection of the expression of GFP-tagged gene products, G418 (Invitrogen) was used at concentration of 400 µg/ml, with subsequent maintenance of the cells at 100 µg/ml G418. pLKO-associated gene products were selected for with puromycin (Invitrogen) at 10 µg/ml and their expression was maintained with 1 µg/ml puromycin.

FFAR4 and FFAR1 vectors and shRNA

shRNA clones for FFAR4 were purchased from Open Biosystem. The sequence encoding the shRNA was 5′-CCGGCCACCTGCTCTTCTACG-TGATCTCGAGATCACGTAGAAGAGCAGGTGGTTTTT-3′. Vectors for FFAR4 and FFAR1 were kindly provided by Gozo Tsujimoto (Hirasawa et al., 2005; Hara et al., 2009). *Nhe*I-*Eco*RI FFAR4-GFP was

cloned into *Xho*I-*EcoR*I pEGFP-C1. The primers were: 5′ *Nhe*I-FFAR4-GFP, 5′-GCCGCCCCGGCTAGCATGTCCCCTGAATGCGCGCGGGCA-3′; 3′ *EcoR*I-FFAR4-GFP, 5′-GCTTCGAATTCTTTACTTGTACAGCT-CGTCCAT-3′. The 5′ primer containing an *Xho*I site for cloning FFAR1 into pEGFP-C1 was 5′-CTCAGATCTCGAGCTGACCTGCCCCCGCAGCT-CTCC-3′. The 3′ primer containing an *EcoR*I site for cloning FFAR1 into pEGFP-C1 was 5′-GCTTCGAATTCTTTACTTCTGGGACTTGCCCCC-3′. Introduction of the R270H mutation into the FFAR4-GFP vector was performed using the 5′ mutating R270H primer 5′-AGCCACCAGATCCA-CGTGTCCCAGCAG-3′ and the 3′ mutating R270H primer 5′-CTGCTGG-GACACGTGGATCTGGTGGCT-3′.

Competing interests

The authors declare no competing interests.

Author contributions

M.J.O.W., S.A.R. and A.R. conceived the project and designed the experimental strategy. A.R. performed the majority of the experiments, S.A.R. also performed experiments and the molecular biology, and Q.Z. performed the mass spectrometric lipid analysis. M.J.O.W., A.R. and S.A.R. wrote the manuscript.

Funding

This work was supported by the European Union FP7 LipidomicNet project; and by the Biotechnology and Biological Sciences Research Council (UK).

References

Agarwal, A. K. and Garg, A. (2006). Genetic disorders of adipose tissue development, differentiation, and death. *Annu. Rev. Genomics Hum. Genet.* **7**, 175-199.

Anderson, N. and Borlak, J. (2008). Molecular mechanisms and therapeutic targets in steatosis and steatohepatitis. *Pharmacol. Rev.* **60**, 311-357.

Andersson, L., Boström, P., Ericson, J., Rutberg, M., Magnusson, B., Marchesan, D., Ruiz, M., Asp, L., Huang, P., Frohman, M. A. et al. (2006). PLD1 and ERK2 regulate cytosolic lipid droplet formation. *J. Cell Sci.* **119**, 2246-2257.

Athenstaedt, K., Zweytick, D., Jandrositz, A., Kohlwein, S. D. and Daum, G. (1999). Identification and characterization of major lipid particle proteins of the yeast Saccharomyces cerevisiae. *J. Bacteriol.* **181**, 6441-6448.

Bell, M., Wang, H., Chen, H., McLenithan, J. C., Gong, D.-W., Yang, R.-Z., Yu, D., Fried, S. K., Quon, M. J., Londos, C. et al. (2008). Consequences of lipid droplet coat protein downregulation in liver cells: abnormal lipid droplet metabolism and induction of insulin resistance. *Diabetes* **57**, 2037-2045.

Blouin, C. M., Le Lay, S., Eberl, A., Köfeler, H. C., Guerrera, I. C., Klein, C., Le Liepvre, X., Lasnier, F., Bourron, O., Gautier, J.-F. et al. (2010). Lipid droplet analysis in caveolin-deficient adipocytes: alterations in surface phospholipid composition and maturation defects. *J. Lipid Res.* **51**, 945-956.

Boström, P., Andersson, L., Li, L., Perkins, R., Højlund, K., Borén, J. and Olofsson, S.-O. (2009). The assembly of lipid droplets and its relation to cellular insulin sensitivity. *Biochem. Soc. Trans.* **37**, 981-985.

Boutet, E., El Mourabit, H., Prot, M., Nemani, M., Khallouf, E., Colard, O., Maurice, M., Durand-Schneider, A.-M., Chrétien, Y., Grès, S. et al. (2009). Seipin deficiency alters fatty acid Delta9 desaturation and lipid droplet formation in Berardinelli-Seip congenital lipodystrophy. *Biochimie* **91**, 796-803.

Brasaemle, D. L. and Wolins, N. E. (2012). Packaging of fat: an evolving model of lipid droplet assembly and expansion. *J. Biol. Chem.* **287**, 2273-2279.

Cheng, J., Fujita, A., Ohsaki, Y., Suzuki, M., Shinohara, Y. and Fujimoto, T. (2009). Quantitative electron microscopy shows uniform incorporation of triglycerides into existing lipid droplets. *Histochem. Cell Biol.* **132**, 281-291.

Clark, J., Anderson, K. E., Juvin, V., Smith, T. S., Karpe, F., Wakelam, M. J. O., Stephens, L. R. and Hawkins, P. T. (2011). Quantification of PtdInsP3 molecular species in cells and tissues by mass spectrometry. *Nat. Meth.* **8**, 267-272

Clément, S., Peyrou, M., Sanchez-Pareja, A., Bourgoin, L., Ramadori, P., Suter, D., Vinciguerra, M., Guilloux, K., Pascarella, S., Rubbia-Brandt, L. et al. (2011). Down-regulation of phosphatase and tensin homolog by hepatitis C virus core 3a in hepatocytes triggers the formation of large lipid droplets. *Hepatology* **54**, 38-49.

Digel, M., Ehehalt, R. and Füllekrug, J. (2010). Lipid droplets lighting up: insights from live microscopy. *FEBS Lett.* **584**, 2168-2175.

Fang, Y., Vilella-Bach, M., Bachmann, R., Flanigan, A. and Chen, J. (2001). Phosphatidic acid-mediated mitogenic activation of mTOR signaling. *Science* **294**, 1942-1945.

Fujimoto, T. and Ohsaki, Y. (2006). Cytoplasmic lipid droplets: rediscovery of an old structure as a unique platform. *Ann. N. Y. Acad. Sci.* **1086**, 104-115.

Fujimoto, Y., Onoduka, J., Homma, K. J., Yamaguchi, S., Mori, M., Higashi, Y., Makita, M., Kinoshita, T., Noda, J., Itabe, H. et al. (2006). Long-chain fatty acids induce lipid droplet formation in a cultured human hepatocyte in a manner dependent of Acyl-CoA synthetase. *Biol. Pharm. Bull.* **29**, 2174-2180.

Fujimoto, T., Ohsaki, Y., Cheng, J., Suzuki, M. and Shinohara, Y. (2008). Lipid droplets: a classic organelle with new outfits. *Histochem. Cell Biol.* **130**, 263-279.

Gaunt, E., Zhang, Q., Cheung, W., Wakelam, M. J. O., Lever, A. and Desselberger, U. (2013). Lipidome analysis of rotavirus-infected cells confirms the close interaction of lipid droplets with viroplasms. *J. Gen. Virol.* **94**, 1576-1586.

Goodman, J. M. (2009). Demonstrated and inferred metabolism associated with cytosolic lipid droplets. *J. Lipid Res.* **50**, 2148-2156.

Griffiths, B., Lewis, C. A., Bensaad, K., Ros, S., Zhang, Q., Ferber, E. C., Konisti, S., Peck, B., Miess, H., East, P. et al. (2013). Sterol regulatory element binding protein-dependent regulation of lipid synthesis supports cell survival and tumor growth. *Cancer and Metabolism* **1**, 3.

Hara, T., Hirasawa, A., Sun, Q., Koshimuzu, T. A., Itsubo, C., Sadakane, K., Awaji, T. and Tsujimoto, G. (2009). Flow cytometry-based binding assay for GPR40 (FFAR1; free fatty acid receptor 1). *Mol. Pharmacol.* **75**, 85-91

Hirasawa, A., Tsumaya, K., Awaji, T., Katsuma, S., Adachi, T., Yamada, M., Sugimoto, Y., Miyazaki, S. and Tsujimoto, G. (2005). Free fatty acids regulate gut incretin glucagon-like peptide-1 secretion through GPR120. *Nat Med.* **11**, 90-94

Hodges, B. D. M. and Wu, C. C. (2010). Proteomic insights into an expanded cellular role for cytoplasmic lipid droplets. *J. Lipid Res.* **51**, 262-273.

Ichimura, A., Hirasawa, A., Poulain-Godefroy, O., Bonnefond, A., Hara, T., Yengo, L., Kimura, I., Leloire, A., Liu, N., Iida, K. et al. (2012). Dysfunction of lipid sensor GPR120 leads to obesity in both mouse and human. *Nature* **483**, 350-354.

Kasai, T., Ohguchi, K., Nakashima, S., Ito, Y., Naganawa, T., Kondo, N. and Nozawa, Y. (1998). Increased activity of oleate-dependent type phospholipase D during actinomycin D-induced apoptosis in Jurkat T cells. *J. Immunol.* **161**, 6469-6474.

Khatchadourian, A., Bourque, S. D., Richard, V. R., Titorenko, V. I. and Maysinger, D. (2012). Dynamics and regulation of lipid droplet formation in lipopolysaccharide (LPS)-stimulated microglia. *Biochim. Biophys. Acta* **1821**, 607-617.

Long, A. P., Manneschmidt, A. K., VerBrugge, B., Dortch, M. R., Minkin, S. C., Prater, K. E., Biggerstaff, J. P., Dunlap, J. R. and Dalhaimer, P. (2012). Lipid droplet de novo formation and fission are linked to the cell cycle in fission yeast. *Traffic* **13**, 705-714.

McDermott, M., Wakelam, M. J. O. and Morris, A. J. (2004). Phospholipase D. *Biochem. Cell Biol.* **82**, 225-253.

Meex, R. C. R., Schrauwen, P. and Hesselink, M. K. C. (2009). Modulation of myocellular fat stores: lipid droplet dynamics in health and disease. *Am. J. Physiol.* **297**, R913-R924.

Nakamura, N., Banno, Y. and Tamiya-Koizumi, K. (2005). Arf1-dependent PLD1 is localized to oleic acid-induced lipid droplets in NIH3T3 cells. *Biochem. Biophys. Res. Commun.* **335**, 117-123.

Neuschwander-Tetri, B. A. (2010). Nontriglyceride hepatic lipotoxicity: the new paradigm for the pathogenesis of NASH. *Curr. Gastroenterol. Rep.* **12**, 49-56.

Norton, L. J., Zhang, Q., Saqib, K. M., Schrewe, H., Macura, K., Anderson, K. E., Lindsley, C. W., Brown, H. A., Rudge, S. A. and Wakelam, M. J. O. (2011). PLD1 rather than PLD2 regulates phorbol ester-, adhesion dependent- and Fcg receptor-stimulated reactive oxygen species production in neutrophils. *J. Cell Sci.* **124**, 1973-1983

Paul, A., Chang, B. H.-J., Li, L., Yechoor, V. K. and Chan, L. (2008). Deficiency of adipose differentiation-related protein impairs foam cell formation and protects against atherosclerosis. *Circ. Res.* **102**, 1492-1501.

Pettitt, T. R., McDermott, M., Saqib, K. M., Shimwell, N. and Wakelam, M. J. O. (2001). Phospholipase D1b and D2a generate structurally identical phosphatidic acid species in mammalian cells. *Biochem. J.* **360**, 707-715.

Robenek, H., Buers, I., Hofnagel, O., Robenek, M. J., Troyer, D. and Severs, N. J. (2009). Compartmentalization of proteins in lipid droplet biogenesis. *Biochim. Biophys. Acta* **1791**, 408-418.

Sato, S., Fukasawa, M., Yamakawa, Y., Natsume, T., Suzuki, T., Shoji, I., Aizaki, H., Miyamura, T. and Nishijima, M. (2006). Proteomic profiling of lipid droplet proteins in hepatoma cell lines expressing hepatitis C virus core protein. *J. Biochem.* **139**, 921-930.

Schadinger, S. E., Bucher, N. L. R., Schreiber, B. M. and Farmer, S. R. (2005). PPARgamma2 regulates lipogenesis and lipid accumulation in steatotic hepatocytes. *Am. J. Physiol.* **288**, E1195-E1205.

Scott, S. A., Selvy, P. E., Buck, J. R., Cho, H. P., Criswell, T. L., Thomas, A. L., Armstrong, M. D., Arteaga, C. L., Lindsley, C. W. and Brown, H. A. (2009). Design of isoform-selective phospholipase D inhibitors that modulate cancer cell invasiveness. *Nat. Chem. Biol.* **5**, 108-117.

Sturley, S. L. and Hussain, M. M. (2012). Lipid droplet formation on opposing sides of the endoplasmic reticulum. *J. Lipid Res.* **53**, 1800-1810.

Tauchi-Sato, K., Ozeki, S., Houjou, T., Taguchi, R. and Fujimoto, T. (2002). The surface of lipid droplets is a phospholipid monolayer with a unique Fatty Acid composition. *J. Biol. Chem.* **277**, 44507-44512.

Thiele, C. and Spandl, J. (2008). Cell biology of lipid droplets. *Curr. Opin. Cell Biol.* **20**, 378-385.

Vereshchagina, N. and Wilson, C. (2006). Cytoplasmic activated protein kinase Akt regulates lipid-droplet accumulation in Drosophila nurse cells. *Development* **133**, 4731-4735.

Walther, T. C. and Farese, R. V., Jr (2009). The life of lipid droplets. *Biochim. Biophys. Acta* **1791**, 459-466.

Wan, H.-C., Melo, R. C. N., Jin, Z., Dvorak, A. M. and Weller, P. F. (2007). Roles and origins of leukocyte lipid bodies: proteomic and ultrastructural studies. *FASEB J.* **21**, 167-178.

Zweytick, D., Athenstaedt, K. and Daum, G. (2000). Intracellular lipid particles of eukaryotic cells. *Biochim. Biophys. Acta* **1469**, 101-120.